Influence of *m*-Isopropenyl-α,α-dimethylbenzyl isocyanate Grafted Polypropylene on the Interfacial Interaction of Wood-Flour/Polypropylene Composites

Chui Gen Guo,[1,2] Qing Wen Wang[2]

[1]*Heilongjiang Key Laboratory of Molecular Design and Preparation of Flame Retardant Materials, College of Science, Northeast Forestry University, Harbin 150040, People's Republic of China*
[2]*MOE Key Laboratory of Bio-Based Material Science and Technology, Material Science and Engineering College, Northeast Forestry University, Harbin 150040, People's Republic of China*

Received 8 June 2007; accepted 2 December 2007
DOI 10.1002/app.27800
Published online 21 May 2008 in Wiley InterScience (www.interscience.wiley.com).

ABSTRACT: In this article, the effects of *m*-isopropenyl-α,α-dimethylbenzyl isocyanate grafted polypropylene (*m*-TMI-PP) on the interfacial interaction of wood-flour/polypropylene (WF/PP) were investigated by means of scanning electron microscopy (SEM), differential scanning calorimetry (DSC), thermogravimetry, dynamic rheological analysis, and mechanical properties tests. The experimental results demonstrated that *m*-TMI-PP greatly improved the interfacial interaction between WF and PP. According to the DSC results, *m*-TMI-PP made the crystallization temperature and the crystallization degree of PP in WF/*m*-TMI-PP/PP decrease when compared with WF/PP composite without *m*-TMI-PP, but it was still higher than pure PP. These results demonstrated that WF presented the nucleate effect for the crystallization of PP and *m*-TMI-PP improved the interfacial adhesive, which restrained the mobility of PP chain. The rheological analysis indicated that the complex viscosity, storage, and loss modular of WF/PP composite increased, and the tan δ decreased with the addition of *m*-TMI-PP. This was attributed to the strong improvement effects of *m*-TMI-PP on the interfacial interaction of the composites, and was further confirmed by the mechanical properties tests and SEM analysis of the composites. © 2008 Wiley Periodicals, Inc. J Appl Polym Sci 109: 3080–3086, 2008

Key words: poly(propylene); interfacial interaction; morphology; rheological behavior; wood flour

INTRODUCTION

In recent years, polymers have replaced many conventional materials, such as metal and wood in many applications. This is due to the advantages of polymers over conventional materials.[1,2] Another product, natural fiber-reinforced polymer, recently attracted the attention of researchers because of its advantages over the materials of its components. Natural fibers are biodegradable and easily available, with the advantages of low cost, low density, lower abrasive, and damage nature to processing equipment as compared with glass-fibers.[3–5] Wood-fiber/thermoplastic composites are environmental friendly and economical, being considered a new way to utilize wood resource effectively,[6–9] and may play an important role in resolving environmental problems arising from solid wastes of wood and plastic products. However, the poor compatibility between the hydrophobic polymer matrix and the hydrophilic wood fiber, the tendency for wood fiber to form aggregates during the processing and the ease to adsorb moisture, greatly reduced the potential of wood fiber to be used as reinforcement for polymers.[10–12]

Generally, the thermoplastic matrix and wood fiber do not interact each other strongly, resulting in poor stress transfer along the interface.[13] The properties of wood-fiber/polypropylene composites were very poor in the absence of interfacial modifiers.[14] Many modification methodologies have been employed to reduce this problem, such as chemical modification of the filler or the addition of compatibilizer to enhance the interfacial compatibility and increase the mechanical and physical properties of polypropylene/wood-fiber composites. Studies showed that the addition of maleic anhydride grafted polypropylene (MAPP) significantly improved the fiber/matrix bonding.[15–18] Isocyanates[19–21] (such as 1,6-diisocyanatohexane, toluene diisocyanate, 4,4′-diphenylmethane diisocyanate) were used as compatibilizing agents in cellulose-based polypropylene composites to improve the interfacial adhesion. A polymeric isocyanate, *m*-isopropenyl-α,α-dimethylbenzyl isocyanate grafted polypro-

Correspondence to: Q. W. Wang (qwwang@nefu.edu.cn).
Contract grant sponsor: National Foundation of Application of Agricultural Scientific and Technological Achievements; contract grant number: 2006GB23600450.
Contract grant sponsor: Heilongjiang Provincial Young Science and Technology Special Foundation of China; contract grant number: QC07C21.

pylene (*m*-TMI-PP), was synthesized and used as compatibilizer in PP/polyamides blends.[22] The improved mechanical properties of wood fiber/PP composite were observed by using *m*-TMI-PP as compatibilizer, and the composite was characterized by mechanical test and FTIR analysis.[23] The interfacial interaction is also very important for improving mechanical properties of wood-flour/polypropylene (WF/PP); however, the interfacial interaction is rarely reported.

In this study, the emphasis was placed on the characterization of interface compatibility between PP and WF using *m*-TMI-PP as compatibilizer. WF/PP composites were prepared by a twin-screw/single-screw extruder system, the effects of *m*-TMI-PP on the interfacial adhesion behavior of WF/PP composites were investigated by morphology, thermal analysis, dynamic rheological analysis, and mechanical tests.

EXPERIMENTAL

Materials

PP (density 0.89–0.91 g/cm^3, the melting flow index of 8 g/10 min at 230°C) used as the matrix of the composites was supplied by DaQing PetroChemical Complex (Daqing, China). WF with 8% content of moisture was supplied by Harbin Yongxu (Harbin, China). *m*-TMI was manufactured by Cytec (Patterson, NJ), dicumyl peroxide (DCP) was manufactured by Tianjin Guangfa (Tianjin, China), *m*-TMI-PP with grafting ratio 1.8% used as compatibilizing agent for WF/PP composites was prepared by our laboratory.

Preparation of composites

WF were dried at 105°C for 24 h for removing moisture and then stored over in sealed containers. A novel compatibilizer (*m*-TMI-PP) with isocyanate functional group was synthesized by grafting *m*-isopropenyl-α,α-dimethylbenzyl isocyanate (*m*-TMI) onto isotactic PP, using DCP as the initiator in a twin-screw extruder. To study the effect of the addition of compatibilizer *m*-TMI-PP on the properties of WF/PP, it was decided to employ a fixed ratio of amount of WF/PP and WF/PP as 40 : 60. WF/PP, WF/PP and 6%-*m*-TMI-PP (WF/*m*-TMI-PP/PP) were used. The mixture of WF, PP, and additives was mixed in a high-speed mixer for 8 min, subsequently melted and extruded by the twin-screw/single-screw extruder system and form sheets for testing. The processing temperature for extrusion was set at 150°C for melting zone, 170–180°C for pumping zone, and 175°C for die zone, respectively. The rotary speed of twin-screw was 100 rpm. 6%-*m*-TMI-PP was chosen to study the properties of composites based on our study, more *m*-TMI-PP did not show any further improvement in the modulus and strength, it is up to the saturation level of the compatibilizer. This was attributed to the plasticization effect of the low-molecular weight *m*-TMI-PP.

Mechanical property tests

Determination of tensile and flexural properties was carried out with a Regeer computer controlled mechanical instrument (produced by Shenzhen Regear Instrument Cooperation), and the test of Izod impact was performed by Unnotched Izod impact instrument, respectively, accordance to ASTM standards. Five specimens of each formulation were tested and the average values were reported.

Scanning electron microscopy

For the observation of interface behavior and dispersivity of WF in WF/PP, specimens were fractured under liquid nitrogen condition. The fracture surface of the sample was sputter-coated with gold layer before examination, and the morphology micrographs of the composites were obtained at magnifications of 3000× using FEI QuanTa200 SEM (Holand), for which the accelerating voltage was 15 kV.

Thermal analysis

Thermal analysis tests were carried out using a Perkin–Elmer Diamond differential scanning calorimetry (DSC) apparatus. All measurements were tested under pure nitrogen gas at a heating rate of 10°C/min. The weight of samples was kept at about 5 mg. The samples were first heated from 25 to190°C and held at this temperature for 5 min to remove their thermal history. The samples were then cooled to 25°C and held for 2 min before reheating to 190°C. The values of crystallization temperature (T_c), melting temperature (T_m), and melting enthalpy (ΔH_m) were determined from the cooling and second heating scans.

Thermogravimetry analysis (TGA), on a Perkin–Elmer Pyris 1Instrument, was performed at a rate of 10°C/min under a nitrogen atmosphere to examine the thermal degradation behavior.

Rheology measurements

Dynamic rheological properties of the composites were measured by TA2000ex rheometer using a parallel plate geometry (2-mm distance of plate-to-plate and 25 mm in diameter). The dynamic strain sweep measurements were carried out first to determine the linear region, four frequencies were chosen, 0.01, 6.28, 62.8, 628 rad/s. The dynamic frequency sweep was then carried out on the samples at the strain of 5% for sample measurements in the linear viscoelastic region at 185°C. The frequency range was 0.01–628 rad/s in a dynamic frequency sweep test with a controlled strain.

TABLE I
Mechanical Properties of WF/PP and its Composites

Sample	Tensile strength (MPa)	Flexural strength (MPa)	Flexural modulus (GPa)	Unnotched Izod impact strength (kJ/m^2)
PP	23.1	29.2	1.3	18.21
WF/PP	29.8	41.3	3.2	10.49
WF/*m*-TMI-PP/PP	39.1	95.8	5.4	13.79

RESULTS AND DISCUSSION

Mechanical properties

The influences of *m*-TMI-PP on the mechanical properties of WF/PP materials are shown in Table I. WF obviously enhanced tensile strength, flexural strength, but decreased unnotched Izod impact strength of WF/PP composite. *m*-TMI-PP with a loading of 6% effectively increased mechanical properties compared with the WF/PP composite. Tensile strength represented an increase of 31.2% from 29.8 to 39.1 MPa, flexural strength exhibited an increase of 132% from 41.3 to 95.8 MPa, and flexural modulus showed an improvement of 68% from 3.2 to 5.4 GPa. This result provided clear evidence that *m*-TMI-PP was an effective interfacial compatibilizing agent for WF/PP composites and increased effectively stress transfer from low-modulus PP to high-modulus WF. So the adding of *m*-TMI-PP improves interface interaction and adhesion between the WF and matrix PP leading to better PP to WF stress transfer. Similar observations were reported by Karmarkar et al.[23] in PP/wood fiber system. These results of mechanical properties are in agreement with following interfacial analysis results.

Morphology observation

The SEM micrographs of the composites (WF/PP, WF/*m*-TMI-PP/PP) are given in Figures 1 and 2, respectively. The micrographs are obtained from cryo-fractured surfaces of the composites. From Figure 1, voids presented around the WF, this result indicates that the interfacial adhesion between PP and WF was very weak due to weakly physical interaction based upon WF break or pullout, which is consistent with the poor mechanical strength.

In Figure 2, the WF was embedded in PP matrix phase, as the rough surface on WF was seen. It was shown that interfacial interaction of WF and PP was improved by *m*-TMI-PP based upon the surface of WF, in which WF are tightly connected with PP matrix. Good adhesion between WF and PP were obtained. Therefore, this result produces a positive effect on the tensile, flexural, and Izod impact strength, which means that loads can be transferred from PP matrix to the WF. This result demonstrates that *m*-TMI-PP improved the interfacial interaction between WF and PP. The improved interfacial adhesion is in agreement with the enhanced mechanical strength as discussed earlier.

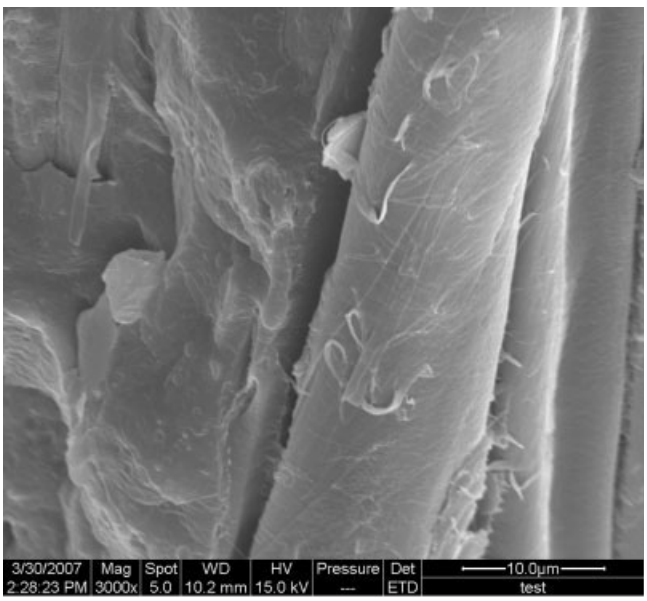

Figure 1 SEM micrographs of WF/PP.

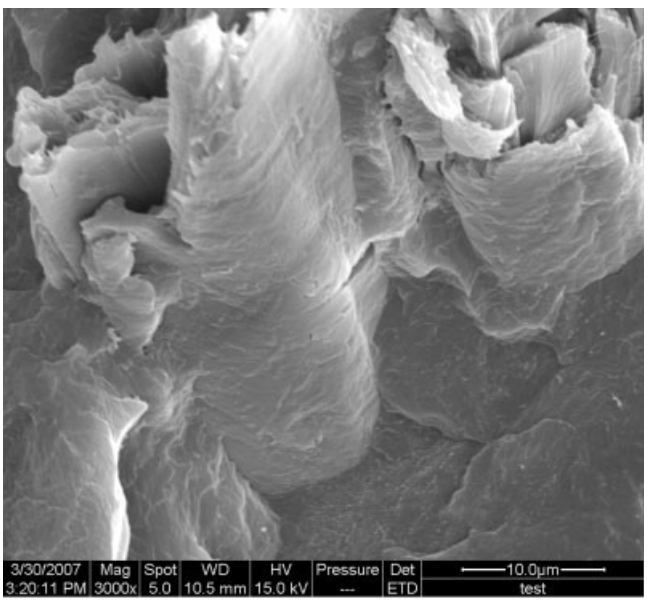

Figure 2 SEM micrographs of WF/*m*-TMI-PP/PP.

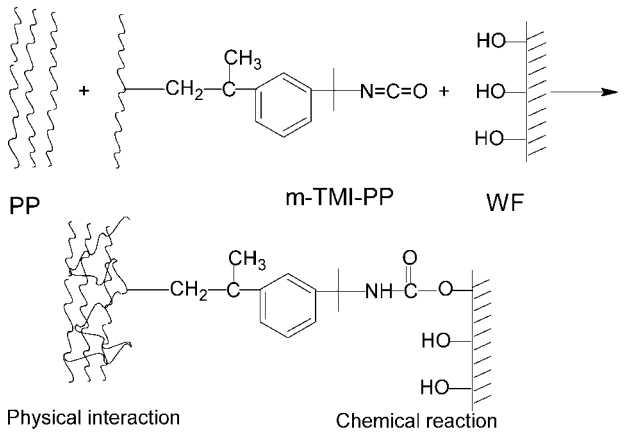

Scheme 1 Schematic hypothesis of interfacial interaction for WF/*m*-TMI-PP/PP.

By considering the mechanical properties and the microstructures, the interaction among WF, PP, and *m*-TMI-PP may be illustrated as in Scheme 1, there is no interaction between WF and PP, which is in agreement with the morphology and the lower mechanical strength. At the presence of *m*-TMI-PP, it was proposed that —NCO group in *m*-TMI-PP molecule reacted with free superficial —OH on the surface of WF to form chemical bond and reduce the polarity as well as the hydrophilicity of WF surface to increase the compatibility of WF and PP, resulting the composite with an enhanced tensile, flexural strength, and improved interfacial adhesion. The —NCO group is highly reactive with the free —OH group of WF, which yields a urethane linkage, and therefore isocyanate is chemically linked to the WF. Therefore *m*-TMI-PP effectively improved the interfacial interaction between PP and WF.

Thermal analysis

The DSC curves of pure PP and its composites during cooling and heating cycles are shown in Figure 3. The

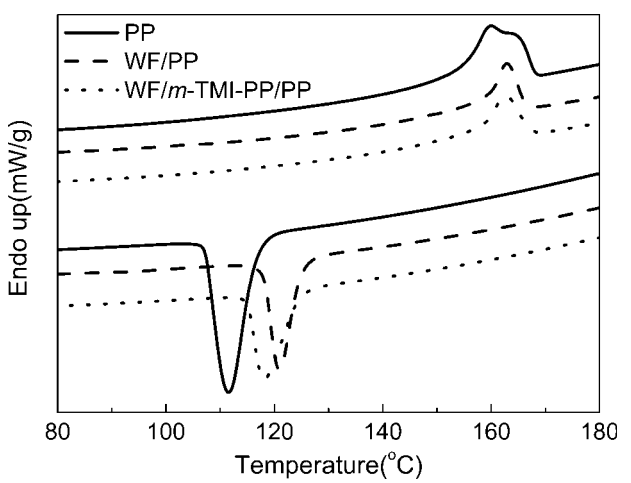

Figure 3 DSC crystallization and melting peak for PP and its composites.

TABLE II
The Thermal Properties of PP and its Composites

Samples	T_m (°C)	ΔH_m (J/g)[a]	T_c (°C)	X_c (%)[b]
PP	159.8/164.2	84.09	111.5	40.23
WF/PP	163.1	104.7	120.9	50.09
WF/*m*-TMI-PP/PP	162.6	88.81	118.2	42.49

[a] Values normalized to the amount of the PP phase.
[b] The X_c is calculated from the ratio of ΔH_m to ΔH_m^0, the ΔH_m^0 of PP with 100% degree of crystallization is 209 J/g.[24]

PP shows a main melting peak and a shoulder at higher temperature, the peak of higher temperature is minor than that of lower temperature. The formation of two melting peaks attributes the secondary crystallization of PP. However, the WF/PP composites show only one melting peak and increased T_m, showing the perfect crystal was formed, the presence of WF in the composites increased the crystallization temperature of PP. This phenomenon supports the role of the nucleating sites, as played by the WF. The thermal parameters, such as crystallization temperature (T_c), maximum melting point (T_m), the heat fusion (ΔH_m), and the crystallinity (X_c), were determined or calculated from the DSC curves, which are summarized in Table II. The T_c of WF/*m*-TMI-PP/PP composites is 2.7°C lower than that of WF/PP, this is the chemical bond between *m*-TMI-PP and WF limit the rearrangement of PP molecules, resulting in the decrease of crystalline temperature of PP in composites, the melt viscosity of WF/*m*-TMI-PP/PP is higher and retard the macromolecule to rearrange regularly to form crystals, which results in the lower X_c and T_m. It was seen that the ΔH_m of WF/PP composite was increased, due to heterogeneous nucleation effect of WF in the system, which promoted the crystallization process of the WF/PP composites. For WF/*m*-TMI-PP/PP composite, a decrease of the ΔH_m and X_c was observed compared with WF/PP, which indicated a reduction of nucleating activity of WF, and further prove the improved interaction between the PP and WF. It was found that the transition temperature corresponding to T_m and ΔH_m in composites increased, but in WF/*m*-TMI-PP/PP, the value of T_m and ΔH_m increased slightly. The result is indicative of interaction between the PP and WF. It is acceptable that the presence of *m*-TMI-PP in the composites disturbs the motion of PP chain and results in a decrease in the crystallization of PP. The thermal data in Table II also implied that the WF/*m*-TMI-PP/PP possessed a stronger interaction between WF and PP.

As seen in Table II, the crystallization temperatures were159.8, 163.1, and 162.6°C for PP, WF/PP, and WF/*m*-TMI-PP/PP, respectively. This result was because the addition of *m*-TMI-PP effectively improved the interface adhesion between PP and WF, and made the PP segment motion become more difficult.

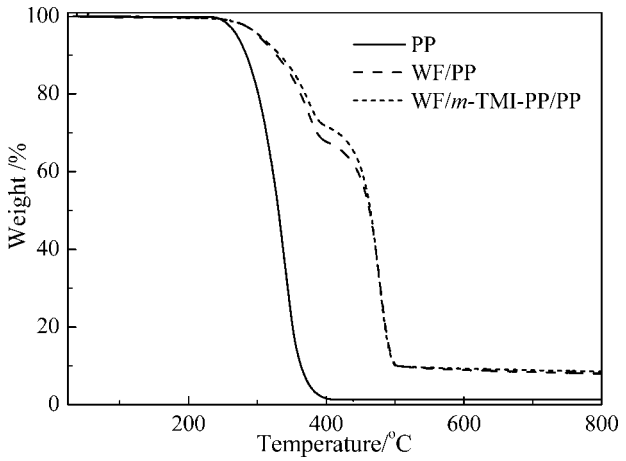

Figure 4 Thermogravimetric analysis of PP and its composites.

The effect of WF and *m*-TMI-PP on the thermal degradation of PP was studied using TGA in the temperature range of 25–800°C, and TGA curves are shown in Figure 4. The initial thermal stabilities are characterized by the temperatures at which 1 and 5% weight losses occurred, referred to as $T_{-1\%}$ and $T_{-5\%}$, respectively (data for the variation in these temperatures are summarized in Table III).From these curves, it can be observed that the thermal degradation of the PP in this temperature range occurs through a one-degradation step. The PP has a sharp decomposition corresponding to the mass loss by the degradation of PP. However, the WF/PP composites in the same temperature range occur through three degradation steps. The TGA curves also indicated that incorporation of WF into the PP improved the thermal stability of composite. Furthermore, compared with the WF/PP at the same weight ratio, the WF/*m*-TMI-PP/PP exhibited slightly higher thermal stability by 2°C. As a result, the WF/*m*-TMI-PP/PP achieves slightly higher thermal stability and char residue than WF/PP.

Rheological behavior

The dynamic viscoelastic measurements were done in linear viscoelastic region at constant temperature of 185°C. To evaluate the linear viscoelastic region (LVE), storage modulus G' and loss modulus G'' were plotted as a function of strain at frequency of 0.01–628 rad/s [Fig. 5(a,b)], because in linear viscoelastic region G' and G'' curves are flat with strain amplitude. In other words, the physical structure of samples does not change with small change in shear deformations.

TABLE III
TGA Data Obtained for the PP and its Composites

Sample	$T_{-1\%}$ (°C)	$T_{-5\%}$ (°C)	Char residue (%) 800°C
PP	249.1	270.6	1.32
WF/PP	258.4	301.6	7.98
WF/*m*-TMI-PP/PP	259.8	303.7	8.49

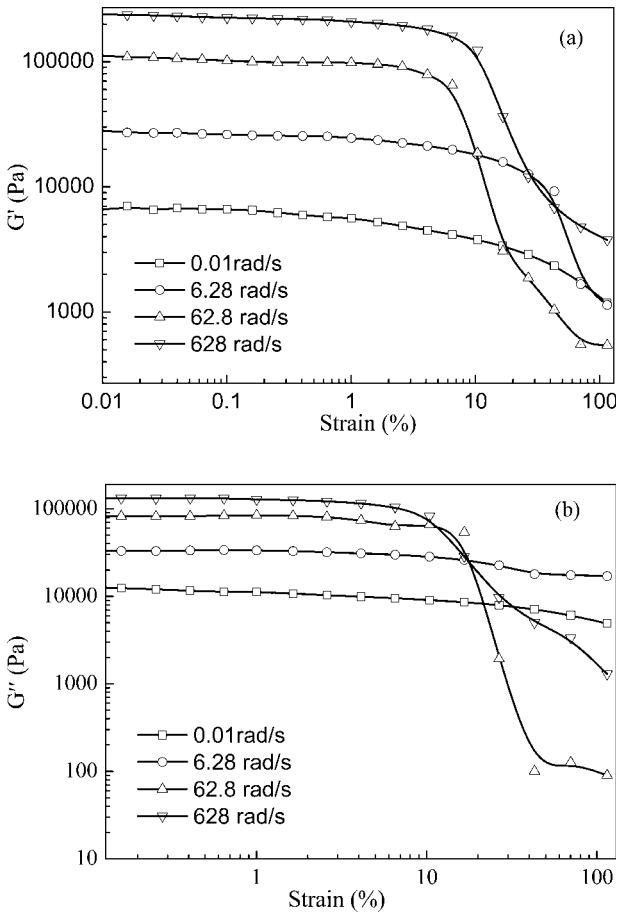

Figure 5 The dynamic strain scan curve of composite at differential frequency.

After a strain sweep test, the test conditions for the frequency sweep can be selected to ensure that the test is really carried out in the LVE range.

Figures 6 and 7 show the variation of storage modulus(G') and loss modulus(G'') as a function of angular frequency (ω) for PP filled with WF with and without *m*-TMI-PP at 185°C. As it is seen, the modulus of both composites are higher than that of pure PP, this is attributed to the nature of WF, by adding *m*-TMI-PP, storage modulus further increases, which is more significant at low frequencies, which was considered to be due to the better compatibility between WF and PP, and less mobility of PP segments, indicating an enhanced stiffness.

Figures 6 and 7 show loss factor (tan δ) and complex viscosity (η*) as a function of angular frequency (ω). Tan δ decrease with increase in angular frequency for PP, WF/PP, and WF/*m*-TMI-PP/PP. With the addition of *m*-TMI-PP, tan δ is decreased and complex viscosity is increased, especially at low frequencies.

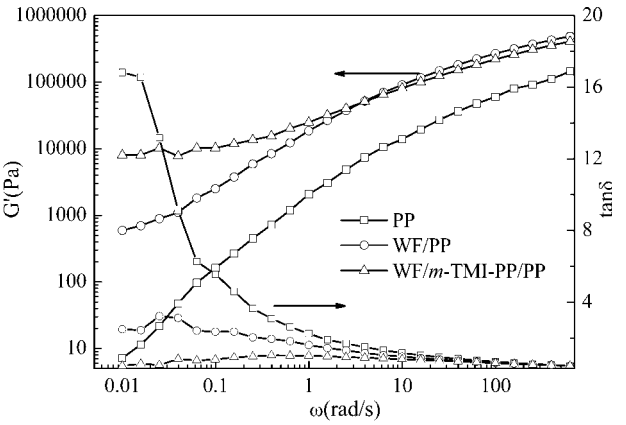

Figure 6 Frequency dependence of dynamic viscoelastic functions (G', tan δ) for PP and its composites at 185°C.

Ashida and Noguchi[24] reported the relation between tan δ and interface adhesion. It can indirectly show the interface adhesion property, the smaller the loss factor tan δ, the better is the interface adhesion. The WF/*m*-TMI-PP/PP-based composites reveals smaller tan δ values and higher storage modulus (G') and complex viscosity, this may all be attributed to the improved interaction at the presence of *m*-TMI-PP, which restrain the PP molecules mobility.

The viscoelastic parameters are improved because of the interaction between PP, WF, and *m*-TMI-PP. Figures 6 and 7 reveals that *m*-TMI-PP change viscoelastic parameters. The WF reduced the mobility of PP chains. Adding *m*-TMI-PP compatibilizing agent reduces the mobility even more because of the effect of formation of strong chemical bonding between the hydroxyl groups of the WF and the isocyanate functional (—NCO) groups, while relying on the chemical similarity of PP and the grafted PP. The PP chains of *m*-TMI-PP may entangle with the matrix PP chains, such as schematic hypothesis in Scheme 1, resulting in effective stress transfer from the PP to WF,[25] which has a result in decreasing tan δ and increasing complex viscosity.

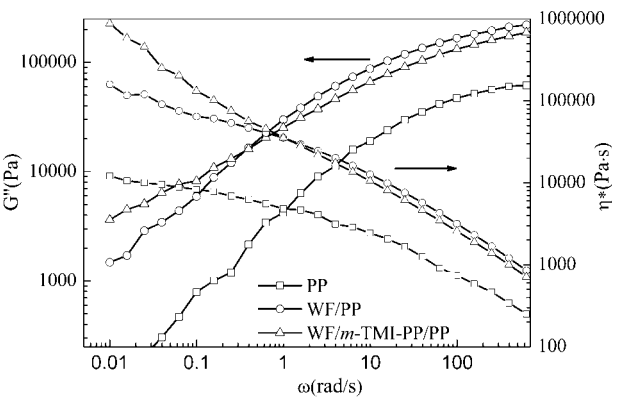

Figure 7 Frequency dependence of dynamic viscoelastic functions (G'', η*) for PP and its composites at 185°C.

CONCLUSIONS

The effects of *m*-TMI-PP on interfacial behavior of WF/PP composites are discussed by SEM, DSC, TGA, dynamic rheological behavior, and mechanical properties. Following conclusions can be drawn:

Compatibilizer *m*-TMI-PP can effectively improve the interfacial interaction between PP and WF. The morphology of WF/*m*-TMI-PP/PP composite indicates that use of *m*-TMI-PP improve adhesion between WF and matrix PP, and hence improving overall properties in the composite. It is proposed that these results are attributed to the chemical reactions of —NCO on *m*-TMI-PP with the —OH groups of WF, and lower molecular chain mobility at the interfacial zone. According to DSC results, *m*-TMI-PP makes PP crystallization temperature and crystallization degree decrease compared with WF/PP composites. The WF/*m*-TMI-PP/PP achieves slightly higher thermal stability and char residue than WF/PP by TGA results.

The rheological property indicates that adding *m*-TMI-PP enhance the viscoelastic properties of composite by easing the transition of stress from WF to the matrix. The smaller tan δ values and higher storage modulus (G') and complex viscosity (η*) proved to be better interfacial adhesion.

All interfacial analysis and mechanical properties obtained in this article indicate that *m*-TMI-PP present the good interfacial interactions between WF and PP.

References

1. Avella, M.; Casale, L.; dell'Erba, R.; Focher, B.; Martuscelli, E.; Marzetti, A. J Appl Polym Sci 1998, 68, 1077.
2. Adrian, J. N.; Pablo, C. S.; Jose, M. K.; Aranguren, M. I.; Norma, E. J Appl Polym Sci 2003, 88, 1420.
3. Georgopoulos, S. Th.; Tarantili, P.A. Polym Degrad Stab 2005, 90, 303.
4. Ismail, H.; Nizam, J. M.; Abdul Khalil, H. P. S. Polym Test 2001, 20, 125.
5. Wielage, B.; Lampke, Th. Mater Process Technol 2003, 139, 140.
6. Suarez, J. C. M.; Coutinha, F. M. B.; Sydenstricker, Th. H. Polym Test 2003, 22, 819.
7. Hristov, V. N.; Vasileva, S. T. Polym Compos 2004, 25, 521.
8. Hristov, V. N.; Vasileva, S. T. J Appl Polym Sci 2004, 97, 1286.
9. Oksman, K.; Clemons, C. J Appl Polym Sci 2003, 67, 1503.
10. Hristov, V. N.; Stefanka, V. Macromol Mater Eng 2003, 288, 798.
11. Hristov, V. N.; Lach, R.; Grellmann, W. Polym Test 2004, 23, 581.
12. Coutinha, F. M. B.; Sydenstricker, Th. H.; Suarez, J. C. M. C.; Melo, D. P. Polym Test 2000, 19, 625.
13. Krzysik, A. M.; Youngqnist, J. A.; Myers, G. E.; Chahyadi, I. S. Wood adhesives. Presented at the Symposium of USDA Forest Service, Madison, WI, 1990. p 183.
14. Karnani, R.; Krishnan, M.; Narayan, R. Polym Eng Sci 1997, 37, 476.

15. Li, H.; Law, S.; Sain, M. J Reinforced Plast Compos 2004, 23, 1153.
16. Hon, D. N. S.; Ren, S. J Reinforced Plast Compos 2003, 22, 957.
17. Guo, C. G.; Wang, Q. W. J Forest Res 2006, 17, 315.
18. Joseph, P. V.; Joseph, K.; Thomas, S.; Pillai, C. K. S. Compos Part A 2003, 34, 253.
19. Qiu, W. L.; Zhang, F. R.; Endo, T.; Hirotsu, T. J Mater Sci 2005, 40, 3607.
20. Nair, K. C. M.; Thomas, S. Polym Compos 2003, 24, 332.
21. Gironès, J.; Pimenta, M. T. B.; Vilaseca, F.; de Carvalho, A. J. F. Carbohydr Polym 2007, 68, 537.
22. Braunn, D.; Schmitt, M. W. Polym Bull 1998, 40, 189.
23. Karmarkar, A.; Chauhan, S. S.; Jayant, M.; Modak, M. C. Compos Part A 2007, 38, 227.
24. Ashida, M.; Noguchi, T. J Appl Polym Sci 1985, 30, 1011.
25. Kawasumi, M.; Hasegawa, N.; Kato, M.; Usuki, A.; Okada, A. Macromolecules 1997, 30, 6333.